International Journal of Waste Resources

OPEN ACCESS Freely available online

Research Article

Efficient Separation of Oil-In-Water Emulsions with Functionalized Superhydrophilic Graphene Oxide-Chitosan Based Composite Membrane

Ponnanikajamideen M[1,2]*, Kai Han[2], Tao Zhou[2]*, Malini M[3], Rajeshkumar S[4]

[1]Environmental Nanotechnology Division, Sri Paramakalyani Centre for Environmental Sciences Manonmaniam Sundaranar University, Alwarkurichi – 627412, Tamilnadu, India; [2]Hunan Provincial Key Laboratory of Efficient and Clean Utilization of Manganese Resources, College of Chemistry and Chemical Engineering, Central South University, Changsha 410083, Hunan, China; [3]Department of Research, Meenakshi Academy of Higher Education and Research, Meenakshi University, Chennai, Tamil Nadu, India; [4]Nanobiomedicine Lab, Department of Pharmacology, Saveetha Dental College and Hospitals, SIMATS, Chennai-600077, TN, Indi

ABSTRACT

Wastewater polluted with oil and other compounds poses enormous threats to the human and environments. Highly efficient separation of "oil" and "water" it is very challenging. The present study focussed on effective method for the separation of emulsified oil using superhydrophilic and superoleophobic cellulose acetate membrane. The membrane was fabricated with graphene oxide (GO) and Chitosan (CS) using vacuum-assisted filtration technique. The modified composite membranes have exceptional separation efficiency. The separation efficiency all the emulsified oils 1:4 concentration is more than 95%, that representing the better "oil" and "water" separation performance. The test of antibacterial activity was performed with gram-positive Bacillus cereus and gram-negative E.Coli was investigated by a zone of inhibition was noted. It is found that Graphene and Chitosan composite membrane have the potential to remove oils from the waste water.

Keywords: Graphene oxide; Chitosan; Membrane; Oil-water separation; Antibacterial

INTRODUCTION

Occasional oil spill accidents, a tremendous increase in industrial wastewater and organic pollutants have produced vulnerable environmental and ecological problems. Nowadays the refinement of oily wastewater has become a worldwide challenging task [1,2]. Hence there is a prerequisite for the development of cost-effective approaches to eradicate the "oil" and "water" mixtures [3,4]. Here to treat the oil-water emulsion, polymer membrane comprises is used due to its smaller pore size than that of oil droplets. Among them, advanced materials with attractive wettability have stimulated many interests, because oil/water separation is operated by interfacial phenomena [6]. The presence of oil contaminants in water can be divided into dispersed oil (20-150 μm), emulsified oil (<20 μm) and free oil (150 μm) based on the size of oil droplets. Among this, the emulsified oil residue is the most difficult type to recycle from the water via conventional methods because of their nano and micro-sized oil droplets [5,7]. In recent years, there have been a large number of artificial hydrophilic and superoleophobic materials that were synthesized via hydrophilic surface modification on polymer membrane [8-10]. However, there is considerable attention paid to membrane technologies to treat the emulsion because of their small marks, high selectivity and low energy cost. In recent times, different super wetting materials were fabricated by crafting surfaces using surface chemistry and modulating roughness [11]. The two types of oil/water separation used to separate wastewater are "removing oil" and "removing water" [5]. Among them, the "removing oil" technique with superhydrophobic and superoleophilic membrane surface have attracted considerable interest. In the oil removal technique, the oil remains to be in the membrane while the water is repelled out. Silica particles layered on stainless steel mesh produce a highly hydrophobic and

***Corresponding to**: Ponnanikajamideen M, Environmental Nanotechnology Division, Sri Paramakalyani Centre for Environmental Sciences Manonmaniam Sundaranar University, Alwarkurichi – 627412, Tamilnadu, India, Tel: +91-50548733; E-mail: ponnanikaja@ymail.com

*Tao Zhou, Hunan Provincial Key Laboratory of Efficient and Clean Utilization of Manganese Resources, College of Chemistry and Chemical Engineering, Central South University, Changsha 410083, Hunan, China, E-mail: zhoutao@csu.edu.cn

Received: March 08, 2021; **Accepted:** Match 11, 2021; **Published:** May 18, 2021

Citation: Ponnanikajamideen M, Kai Han, Tao Zhou, Malini M and Rajesh kumar S (2021) Efficient Separation of Oil-In-Water Emulsions with Functionalized Superhydrophilic Graphene Oxide-Chitosan Based Composite Membrane. Int J Waste Resour 11: 411.

superoleophilic surface for oil-water separation [12].

Graphene oxide (GO) is two-dimensional materials having oxygenated graphene sheets containing carboxyl, hydroxyl, and epoxide functional groups [13]. Therefore, the nano-channel within GO-based membranes can be precisely synchronized and optimally incorporated with functional surfaces of secondary nanomaterials [14]. It is found that the graphene and chitosan composite membrane can remove oils from the wastewater. Chitosan (CS) is a naturally occurring biodegradable material which is non-toxic and biocompatible, it is a polysaccharide produced from the deacetylation of chitin with its hydroxyl and amino functional groups on the surface [15,16].

In this work, we report the synthesis and performance evaluation of GO/CS composite based membranes that have good stability as well as high separation efficiency. A facile vacuum filtration process is employed to achieve large surface area membranes. The composite membranes can separate oil-water emulsions with more than 95% efficiency and interestingly we discovered that the GO/CS composite exhibited strong antibacterial activity against gram-positive *Bacillus cereus* and gram-negative *E.Coli*.

MATERIALS AND METHODS

Materials

Chitosan was purchased from Sigma Aldrich. The pristine cellulose membrane was obtained from the Haining Yanguan filter materials factory (Zhejiang, China). Sodium dodecyl sulphate (SDS), acetic acid, octane, silicone oil was procured from Sinopharm reagent Co-Ltd (Shanghai, China). Soybean oil was locally purchased. All the other reagents used in this study were of analytical grade; all the solutions were prepared using double distilled water.

Fabrication of GO/CS Membrane

The GO/CS modified membranes were synthesized by the filtration method using a vacuum filtration apparatus. 10 mg of GO homogeneous solution was prepared in distilled water by gentle stirring at room temperature. The chitosan solution was prepared by adding 1g of Chitosan into 100 mL of distilled water which was followed by the addition of 0.5 mL glacial acetic acid under the constant stirring condition for an overnight period. The modified GO/CS membrane was denoted as (1:1), (1:2), (1:4), (1:6). The GO concentration was 1.5mg for each modified membrane, and the Chitosan concentration was 1.5 mg, 3.0 mg, 6.0 mg, and 9.0 mg respectively. The prepared GO/CS solution was poured into the filtration device containing a piece of commercial cellulose acetate membrane on the bottom. The cellulose acetate membrane surface was layered with GO/CS membrane with the exposure of nitrogen gas for 30 min after exposure of nitrogen gas for 30 min. Then the membrane was dried at 60^{0}C overnight.

Characterization

The microstructures of the GO/CS membrane were determined by Scanning Electron Microscope (Nova Nano SEM 230). Fourier transform infrared spectroscopy (FTIR) Spectra of GO/CS was performed in the range of 400-4000 cm^{-1}. The crystal peak range was examined by X-ray diffraction (XRD, Japan Rigaku D/MAX-2500). The chemical composition of the membranes was obtained by X-ray photoelectron spectroscopy (XPS, Thermo Fisher ESCALAB 250 XI system). The thermal stability of GO/CS composite was measured by the Thermogravimetric analyser (TGA).

Preparation of Oil-in-Water Emulsions

For this study variety of surfactant-stabilized oil-in-water emulsion (Soybean-and-water, Silicone-and-water, and Octane-and-water) were prepared by adding 10 g of oil in 500 mL of deionized water and then blended with 0.05g of sodium dodecyl sulphate (SDS as the emulsifier). The mixture was stirred by a homogenizer (YING TAI-Instrument TG 20C) at 8000 rpm for 20 min to attain a creamy solution. The prepared emulsions were stored at room temperature and were used for the separation of "oil" and "water".

Oil-Water Separation

The oil-water separation process was done by using the vacuum filtration set up. The separation mechanism is schematically presented in Figure S1. For each separation process, 100 mL of surfactant stabilized oil-in-water emulsion was poured into the filtration cup while maintaining a pressure difference of 0.09 MPa. The vacuum filtration pump was used to pass the water through the membrane into the filtration cup, resulting in the retention of oil droplets on the membrane surface.

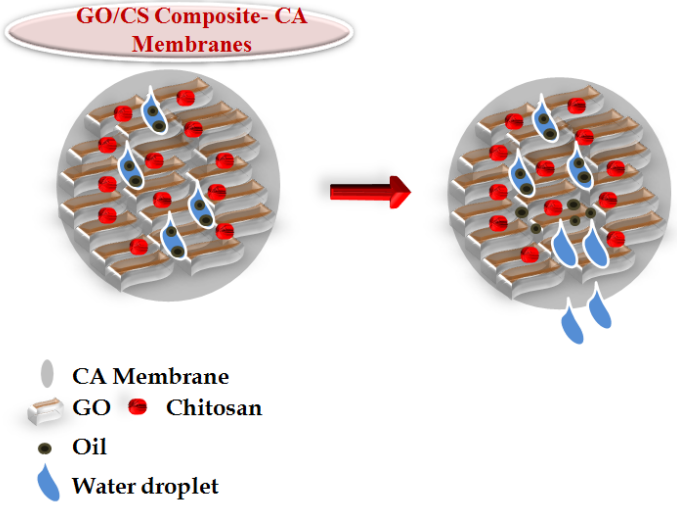

Figure S1: A schematic diagram of the process of oil-water separation, water is able to permeate through the membrane but the oil cannot.

Assay of Antimicrobial Activity

The antimicrobial assay of Graphene – chitosan Membrane was examined by the disk diffusion method (membrane pieces act as a disk). Fresh overnight culture of gram-positive Bacillus cereus and gram-negative *E.Coli* was collected from Meenakshi Academy of Higher Education and Research, Chennai, India. The microorganisms (gram-positive *Bacillus cereus* and gram-negative *E.Coli*) were cultured in Muller Hinton agar and 24 hrs old cultured were swabbed on each plate. A bit of the membrane (20 mm diameter membrane disk) was placed on the center of the incubated plate. After 24 h of incubation at 37°C, the zone of incubation was observed.

RESULTS AND DISCUSSION

Fourier Transform Infrared (spectroscopy)

FTIR spectra analysis was carried out to confirm the formation of GO, CS and GO/CS composite was shown in Figure 1. The

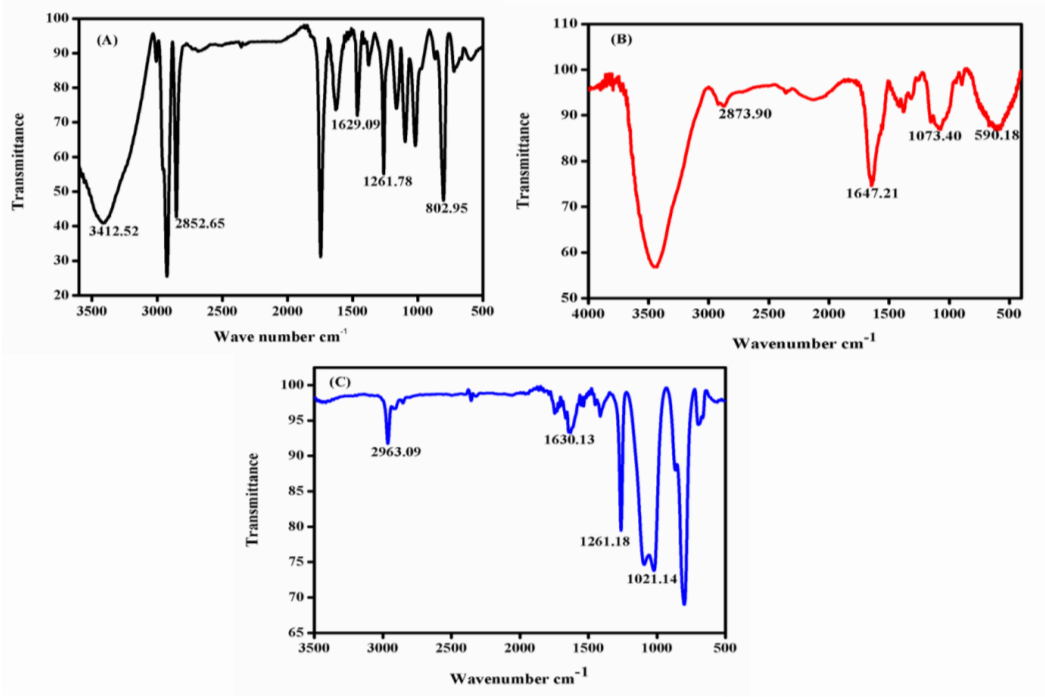

Figure 1: FTIR spectra of GO (A), CS (B) and GO/CS (C) composite.

spectra of GO shows a typical peak at 3412 cm^{-1} here the stretching vibration is the OH group and the peak of 2852 cm^{-1} represents the stretching vibration of the C=O group. In addition, there were two characteristic bands centered at 1629 cm^{-1}, 1261 cm^{-1} denoted C=O stretch and C-H groups respectively. The CS spectra show a peak at 2873 cm^{-1} which demonstrates the C=O stretch. While the peak at 1647 cm^{-1} corresponds to C-C=C group symmetric stretch, the peak at 1073 cm^{-1} represents the C-O group stretch. The FTIR spectrum of GO/CS composite found that the peak at 2963 cm^{-1}corresponds to the stretching vibration of H-C-H asymmetric group, and the peak at 1630 cm^{-1} denoted the C-C=C group symmetric stretch, while the peak at 1261 cm^{-1} shows the presence of C-H group the bond formation of C-H group with CS which was shifted in to 1073.40 for GO/CS. The above adsorption peaks also formed in the FTIR spectrum of GO, CS, and GO/CS composite.

XRD

XRD patterns indicate the crystallinity and nature of the interactions between components of the prepared composites (Figure 2). The simple patterns of different components are contained in there is no chemical interaction between the composites. The different components in the prepared composite showed their own crystal region [17]. The XRD graph of GO has two pointed peaks at 10.0^0 and 20.0^0 (at 2θ) respectively which indicates the interlayer spacing of graphite (002) these spacing due to the oxygen functional group of GO as well as water molecules present in the GO. The XRD pattern of CS shows two peaks at 10.5^0 and 20.5^0 which are linked with the hydrated crystalline structure the broadening of the peaks is due to the amorphous nature of the polymer [18] there are no impurity peaks observed in the XRD Pattern (JCPDS 039-1894) and the peaks at 30.9^0 are correlated to the unstructured nature of the CS composite. In an evaluation of GO and GO/CS the disappearance of peaks at 10.0^0indicate exfoliation of GO into the CS surface. In the XRD pattern of GO/CS, the peaks at 8.5^0 and 10.5^0 are related to the CS 10.5^0 and 20.5^0 GO 10.0^0 and 20.0^0. But the peaks in CS result in significant broadening which suggests a structural disorder [19].

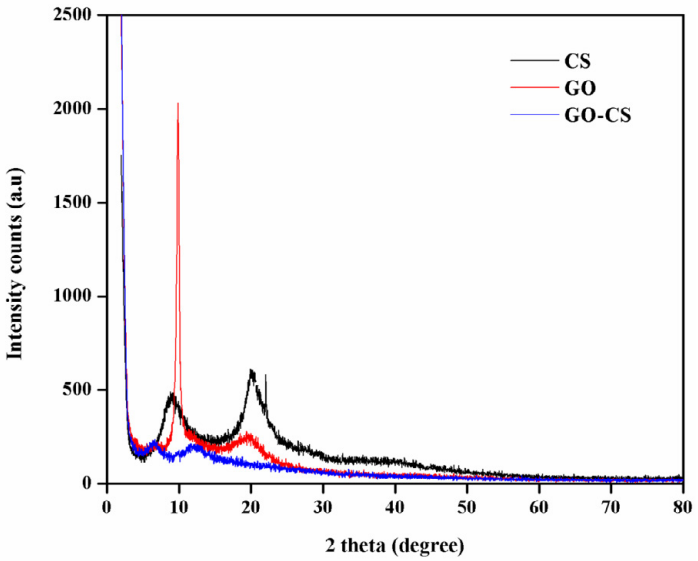

Figure 2: XRD patterns of GO, CS and GO/CS composites.

SEM

SEM images of pristine cellulose acetate membrane and modified membranes by graphene oxide and chitosan are shown in (Figure 3A) which clearly shows that the pristine cellulose membrane has a rich porous arrangement with a comparatively even and clear surface. In (Figure 3B) shows the image of the raw composite material of GO/CS which posses an anisotropic structure. After coating a layer of GO/CS (Figure 3C & D) the composite was found to be uniformly dispersed on the membrane without any agglomeration. The GO/CS modified membrane was smooth and had a clear surface. It also showed the larger roughness due to the coverage of a composite.

TGA

The TGA curves of GO modified with CS composites are presented in Figure 4. Here the weight loss occurred in the range of 150-

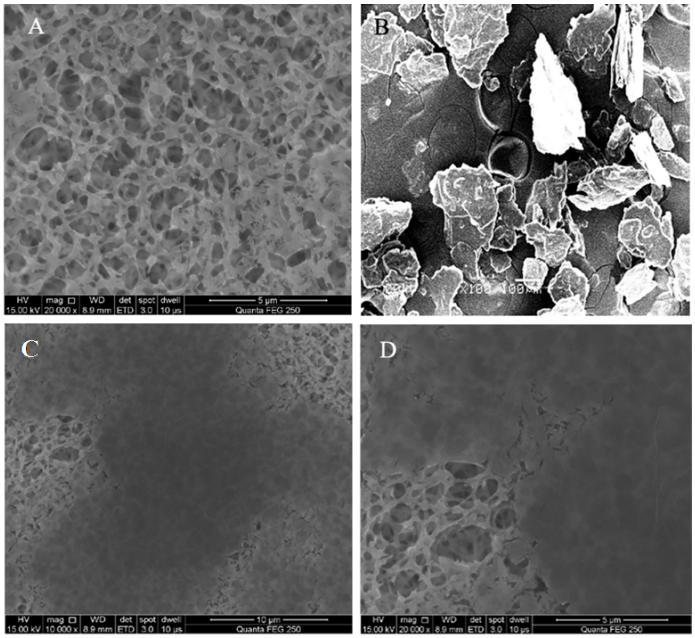

Figure 3: Different magnification of SEM images (A), pristine cellulose membrane (B), raw GO/CS composite material (C, D) GO/CS coated cellulose membrane.

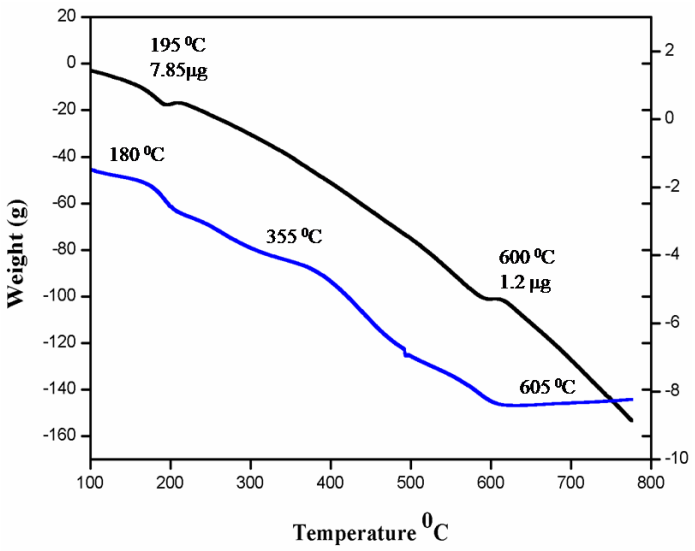

Figure 4: TGA curve for GO/CS composite.

200°C due to dehydration and release of the oxygen molecule the weight loss of about 10 %. The gradual weight loss was observed in the range of 100-800°C However, the major weight loss was seen in the range of 200-650 °C the weight loss of about 40 %. The DTA curve of GO/CS was taken in the temperature range of 150-600 °C. Here a narrow peak at 500 °C corresponds to the decomposition of composite materials and can be attributed to the weight loss of the mixed composition of GO and CS.

XPS

The chemical compositions of each membrane were identified by XPS. Preliminary analysis scans were taken between 0 and 1400 eV binding energy for GO, CS and GO/CS membrane (Figure 5 a-d). The GO spectrum was analyzed for five types of the carbon atom. The peak assigned at 284.5, 286.8, 288.3, and 288.3 eV corresponds to C-OH, C-O, C=O and C (O) O groups, respectively. The first peak at 284.5 eV represents the C-C and C=C bonds [20,21]. The GO survey scan was taken between 0 and 1400 eV binding energy (Figure 5b). The XPS spectrum of the CS membrane denotes the presence of C-C, C-O and C=O groups at 284.5, 285.3 and 287.1 eV respectively. The XPS results of GO/CS membranes point out the presence of C=C/C-C, C-O and C=O groups at 284.6, 285.4 and 287.2 eV respectively [22] which suggest the mass concentration of CS solution, when compare to the GS solution. These results suggest controlling the relation between the CS polymer and GO solution. It was found, that the GO volume is constant and the CS solution mass concentration is different in the prepared membranes. The previous results propose that the oxygen-containing functional groups are often positioned at the edges, with some portion of the functional groups positioned on the surfaces [23].

Oil contact angle

Oil contact angle tests on the surface of GO/CS membrane (1;4) is superhydrophilic and underwater superoleophobic. Here the CA with high-speed camera system is used to document the spreading process of a water droplet there was used to investigate the wetting performance of water on the GO/CS membrane as (Figure 6A, B) shows the 0° water contact angle and underwater oil contract angle are acquire. (Figure 6C, D) shows a water droplet thicken as soon as when it comes in contact with the membrane surface and

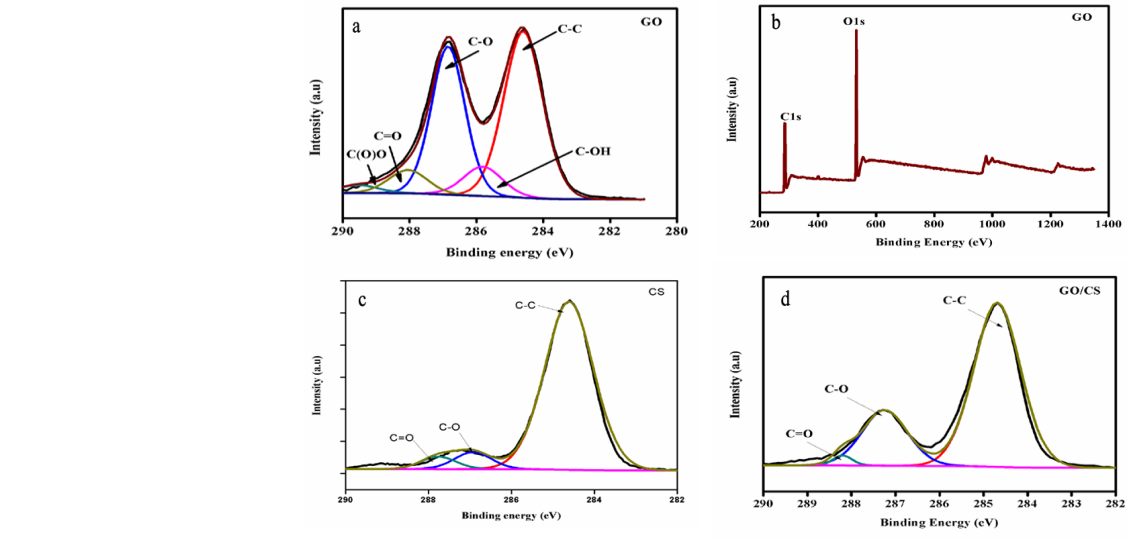

Figure 5: XPS spectrum of GO, CS and GO/CS membranes.

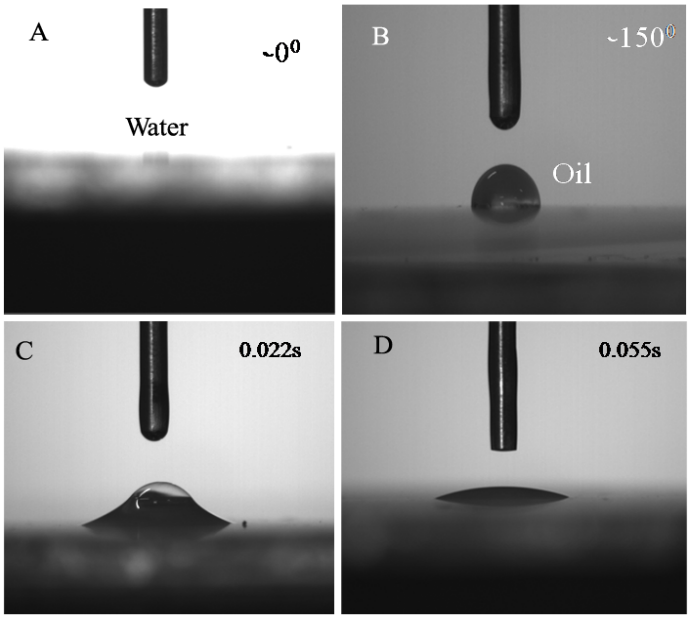

Figure 6: Contact angel for prepared GO/CS (1; 4) concentration membrane.

the whole process completed within 0.1s which shows the better property of wetting. Membrane surface possessions are good for water permeation as refuse oil [25].

Oil water Separation

The oil-water separation of prepared GO/CS membrane was carried out at 0.09 MPa by a vacuum -driven filtration process using different kinds of surfactant-stabilized oil-and-water emulsions which include soybean-and-water, silicone-and-water, and octane-and-water (Figure 7A, B). The membrane was fixed in the dead-end filtration system. Each membrane was first precompacted at specific operating pressure with ultrapure water until it reaches a stable permeate flux, and then the oil-in-water emulsion content was transferred into the filtration system. Here, the emulsion was added, into the system under constant pressure to ensure the smooth flow of water while the oil was retained above the membrane which shows the effective separation of the emulsion. An optical microscope was used to examine the droplets in soybean-and-water emulsion and permeate to further confirm the good separation efficiency of GO/CS membrane for surfactant-stabilized oil-and-water emulsion [24]. However, the oil droplet size was extensively decreased when the surfactant was supplemented, and the normal size of the droplet was approximately 200 nm (Figure 7C). After the separation process, no droplets were found in the collected water (Figure 7D) which confirms the GO/CS membrane is highly proficient for separating oil-in-water emulsion.

The cyclic oil-water separation was performed using a vacuum filtration setup. Before the separation process, the membrane was drenched with water and then inserted between two glass plates. For the separation process, initially, the vacuum pump was switched on, and then 100 mL of the oil-water emulsion was passed through the GO/CS membrane to separate the "oil" and "water". After each surfactant-stabilized emulsion separation process, the used membrane was washed with water. The oil rejection coefficient *R* (%) was calculated by equation [1]

$$R = \left(1 = \frac{cp}{co} \times 100\right) \quad (1)$$

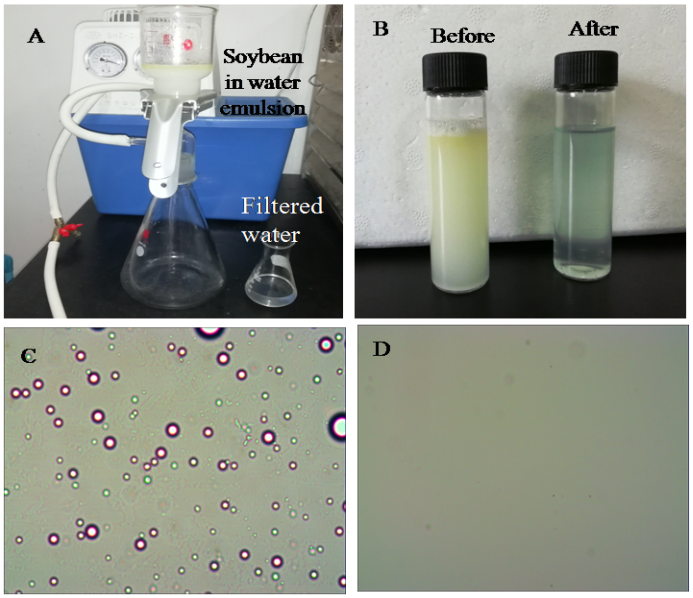

Figure 7: A Separation of Soybean-in-water emulsion with the GO/CS membrane, B shows the emulsion before and after separation. C and D, shows the optical microscopy images of soybean in water emulsions before and after oil water separation with the GO/CS membrane.

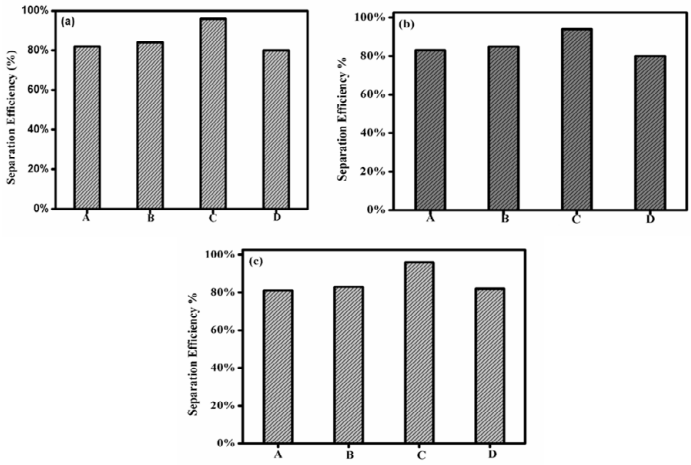

Figure 8: Separation efficiency of different modified membrane (a) Soybean-in-water, (b) silicone-in-water, (c) Octane-in-water; A, modified membrane with (1;1) B (1;2) C (1;4) D (1;6).

Where $C_0$and $C_p$is the concentration of oil in the original oil-and-water emulsion and in the permeate solution respectively. The rejection rate of the emulsion was observed to be more than 95%, as determined by UV-vis spectrophotometer. The separation efficiency of this membrane with different oil-and-water emulsion is shown in (Figure 8). Here, the membrane reveals extremely high separation efficiency of more than 95% with all the investigated surfactant-stabilized oil-and-water emulsion. The GO/CS modified membranes used in the present study were based on varying concentrations and divided into four groups like 1:1, 1:2, 1:4, and 1:6. The 1:4 membranes showed better efficiency in oil-water separation, including 96% in soybean-in-water (Figure 8A), 95% in silicone-in-water (Figure 8B) and 97% in octane-in-water (Figure 8C). Moreover, the adsorbed water layer makes room for the water droplets from the oil-and-water emulsion to the opposite side of the modified membrane. Thus, the oil-and-water emulsion was successfully separated due to the thin water layer that can prevent oil droplets from passing through the modified membrane.

Antimicrobial Assay

Graphene – chitosan membranes are emerging with a wide range of enormous archiving applications. Here we examined the antibacterial activity of graphene – chitosan membranes using gram-positive *Bacillus cereus* and gram-negative *E.Coli* tests, and was investigated for the zone of inhibition. The formation zone was clearly observed around the disk containing graphene-chitosan indicating the antimicrobial nature of the fabricated membranes. The results showed a zone of inhibition of *Bacillus cereus* and *E.Coli* to be 16.2 mm and 19.3 mm, respectively at 20 mm diameter disk. These results were an indication that the Graphene –chitosan membrane had good cytotoxicity action against bacteria. The higher zone of inhibition noted on gram-negative *E.coli* bacteria could be attributed to the fact that the graphene/chitosan membrane could penetrate the cellular membrane of *E.coli* through its sharp edges [26]. This showed that the fabricated graphene Chitosan membrane has the potency to suppress the growth of *E.coli* cells. *E.coli* bacteria get easily attached to the graphene/chitosan membrane which results in the penetration of graphene/chitosan into bacteria causing the intracellular damage and loss of integrity of microorganisms cell membranes [27,28]. This demonstrates that graphene-based material could also kill gram-positive microorganisms and the asymmetry in the result of antibacterial activity can be related to their different cell wall nature. *Bacillus cereus* has a massive peptidoglycan layer while *E.coli* has a delicate type of peptidoglycan layer between the inner and outer cell membranes of microorganisms. Further, we believe that the graphene–chitosan membrane could prevent microorganisms from adhering to the membrane surface, which would be useful for making the membrane good in antimicrobial and antifouling performance.

CONCLUSIONS

In summary, we fabricated GO/CS composite modified membranes with good stability, high separation efficiency and good hydrophilic properties by the filtration technique. This membrane separates the oil-water emulsion with more than 95% efficiency. The hydrophilic GO/CS membrane showed good anti-oil-fouling and very low oil adhesion properties which we believe is an effective method for removing emulsified oils in an industrial setup. The antibacterial properties with gram-positive *Bacillus cereus* and gram-negative *E.Coli* were investigated by a zone of inhibition was noted. Here the results were found that higher zone was noted on *Bacillus cereus* 16.2 mm and the great zone was noted on *E.Coli* 19.3 mm at 20 mm diameter disk. We believe this membrane is effective for applications involving the removal of oily water from industrial wastewater and huge water oil spills, mainly those stabilized by surfactants.

ACKNOWLEDGEMENTS

This work was financially supported by the National Natural Science Foundation of China (21706292) and Hunan Provincial Natural Science Foundation of China (No. 2017JJ3376, 2018JJ2484). K. Han and S. Wang thank the support from the Hunan Provincial Science and Technology Plan Project, China (No. 2016TP1007). Ponnanikajamideen M is funded by postdoctoral foundation from Central South University.

REFERENCES

1. Cheng Y, Li X, Xu Q, Garcia-Pineda O, Andersen OB, Pichel WG. SAR observation and model tracking of an oil spill event in coastal waters. Mar Pollut Bull. 2011;62:350-363.
2. Al-Majed AA, Adebayo A, Hossain ME.A sustainable approach to controlling oil spills. J Environ Manage.2012;113:213-227.
3. Wang B, Liang W, Guo Z, Liu W. Biomimetic super-lyophobic and super-lyophilic materials applied for oil/water separation: a new strategy beyond nature. Chem Soc Rev.2015; 44: 336-361.
4. Xue Z, Cao Y, Liu N, Feng L, Jiang L. Special wettable materials for oil/water separation. Journal of Materials Chemistry A. 2014;2:2445–2460.
5. Pan S, Guo R, Xu W. Durable superoleophobic fabric surfaces with counterintuitive superwettability for polar solvents. AIChE Journal. 2014;60(8):2752-2756.
6. Dunderdale GJ, Urata C, Sato T, England MW, Hozumi A. Continuous, high-speed, and efficient oil/water separation using meshes with antagonistic wetting properties. ACS applied materials & interfaces. 2015 Sep 2;7(34):18915-9.
7. Fan JB, Song Y, Wang S, Meng J, Yang G, Guo X, et al. Directly coating hydrogel on filter paper for effective oil–water separation in highly acidic, alkaline, and salty environment. Advanced Functional Materials. 2015 Sep;25(33):5368-75.
8. Liu M, Li J, Guo Z. Polyaniline coated membranes for effective separation of oil-in-water emulsions. Journal of colloid and interface science. 2016;467:261-70.
9. Wang Z, Jiang X, Cheng X, Lau CH, Shao L. Mussel-inspired hybrid coatings that transform membrane hydrophobicity into high hydrophilicity and underwater superoleophobicity for oil-in-water emulsion separation. ACS applied materials & interfaces. 2015;7(18):9534-45.
10. Shi H, He Y, Pan Y, Di H, Zeng G, Zhang L, et al. A modified mussel-inspired method to fabricate TiO2 decorated superhydrophilic PVDF membrane for oil/water separation. J Membrane Science. 2016;506:60-70.
11. Li J, Zhao Z, Li D, Tian H, Zha F, Feng H, et al. Smart candle soot coated membranes for on-demand immiscible oil/water mixture and emulsion switchable separation. Nanoscale. 2017;9(36):13610-13617.
12. Li B, Liu X, Zhang X, Chai W. Stainless steel mesh coated with silica for oil–water separation. European Polymer J. 2015;73:374-9.
13. Krishnamoorthy K, Veerapandian M, Yun K, Kim SJ. The chemical and structural analysis of graphene oxide with different degrees of oxidation.Carbon. 2013 Mar 1;53:38-49.
14. Zhao X, Su Y, Liu Y, Li Y, Jiang Z. Free-standing graphene oxide-palygorskite nanohybrid membrane for oil/water separation. ACS applied materials & interfaces. 2016;8(12):8247-8256.
15. Chaudhary JP, Vadodariya N, Nataraj SK, Meena R. Chitosan-based aerogel membrane for robust oil-in-water emulsion separation. ACS applied materials & interfaces. 2015;7(44):24957-24962.
16. Mokhena TC, Luyt AS. Development of multifunctional nano/ultrafiltration membrane based on a chitosan thin film on alginate electrospun nanofibres. J Cleaner Production. 2017;156:470-479.
17. Zhuang PY, Li YL, Fan L, Lin J, Hu QL. Modification of chitosan membrane with poly (vinyl alcohol) and biocompatibility evaluation. Int J Biolo Macromolecules. 2012;50(3):658-663.
18. Rhim JW, Hong SI, Park HM, Ng PK. Preparation and characterization of chitosan-based nanocomposite films with antimicrobial activity. J Agricultural Food Chemistry. 2006;54(16):5814-22.
19. Abolhassani M, Griggs CS, Gurtowski LA, Mattei-Sosa JA, Nevins M, Medina VF, et al. Scalable chitosan-graphene oxide membranes: the

effect of GO size on properties and cross-flow filtration performance. ACS omega. 2017;2(12):8751-8759.

20. Park aS, Dikin DA, Nguyen ST, Ruoff RS. Graphene Oxide Papers Modified by Divalent Ions—Enhancing Mechanical Properties via Chemical Cross-Linking. J Phys Chem C. 2009;113:15801-15804.
21. Sobon G, Sotor J, Jagiello J, Kozinski R, Zdrojek M, Holdynski M, et al. Graphene oxide vs. reduced graphene oxide as saturable absorbers for Er-doped passively mode-locked fiber laser. Optics express. 2012;20(17):19463-73.
22. Han D, Yan L, Chen W, Li W. Preparation of chitosan/graphene oxide composite film with enhanced mechanical strength in the wet state. Carbohydrate Polymers. 2011;83(2):653-8.
23. Sun P, Zheng F, Zhu M, Song Z, Wang K, Zhong M, et al. Selective trans-membrane transport of alkali and alkaline earth cations through graphene oxide membranes based on cation–π interactions. Acs Nano. 2014;8(1):850-9.
24. Sun P, Zhu M, Wang K, Zhong M, Wei J, Wu D, et al. Selective ion penetration of graphene oxide membranes. ACS nano. 2013;7(1):428-37.
25. Gao P, Liu Z, Sun DD, Ng WJ. The efficient separation of surfactant-stabilized oil–water emulsions with a flexible and superhydrophilicgraphene–TiO 2 composite membrane. J Materials Chem A. 2014;2(34):14082-14088.
26. Hu W, Peng C, Luo W, Lv M, Li X, Li D, et al. Graphene-based antibacterial paper. ACS Nano. 2010;4(7):4317-4323.
27. Akhavan O, Ghaderi E. Toxicity of graphene and graphene oxide nanowalls against bacteria. ACS Nano. 2010;4(10):5731-5736.
28. Park S, Mohanty N, Suk JW, Nagaraja A, An J, Piner RD, et al. Biocompatible, robust free-standing paper composed of a TWEEN/Graphene composite. Advanced Materials. 2010;22(15):1736-1740.